The effect of Varying the Ratio x on the Electrical and Dielectric Properties of $(ZnFe_2O_4)_x$/ $SiO_{2\ (1-x)}$ Nanocomposites

N.M. Shash , M.H. Makled, M.G. EL-Shaarawy and F.A. Afifi

Department of Physics, Faculty of Science, Benha University, Egypt
nab_shash@yahoo.com

Samples of varying x $(ZnFe_2O_4)$/ (1-x) SiO_2 (where x= 0.4, 0.6 and 0.8) nanocomposites were prepared by sol-gel method. The influence of $ZnFe_2O_4$ content on the structural, electrical and dielectric properties of the nanocomposites was studied. The samples were characterized by X-ray diffraction (XRD), thermogravimetric analysis (TGA) and differential thermal analysis (DTA). The XRD spectra showed that, Zn-ferrite particle size lies in the range of 5.17-34.6 nm. Electrical conductivity of the samples increases as the temperature increases indicating that the samples have semiconductor like behavior. It is also found that the electrical resistivity and dielectric constant of the samples changes considerably with zinc-ferrite content and the sintering temperatures. The variation of electrical resistivity and dielectric constant with zinc-ferrite content are found to be opposite to each other. The possible mechanism for the influence of $ZnFe_2O_4$ content on the electrical properties is discussed in this paper.

1. Introduction:

Polycrystalline spinel ferrites have very good electrical properties that are dependent on several factors such as chemical composition, the method of preparation, and substitution of different cations, etc. Among spinel ferrites, zinc ferrite is one of the most versatile and technologically important ferrite materials because of its high electrochemical stability, catalytic behavior and low conductivity **[1]**.

Zinc is known to play a decisive role in determining the ferrite properties **[2]**. The redistribution of metal ions over the tetrahedral and octahedral sites in the spinel lattice on incorporation of zinc is responsible for the modification of ferrite properties. The properties of ferrites are also sensitive to their composition and microstructure, which in turn are dependent on the method of processing **[3]**.

Various synthetic routes have been reported in the literature for the preparation of nanoscale ferrites such as ceramic method **[4]**, sol-gel **[5]**, co-precipitation **[6]**, solvent evaporation **[7]**, hydrothermal **[8]**, combustion **[9]**, micro emulsion **[10]** and citrate methods **[11]**. Among various synthetic routes, the sol-gel process offers some advantages. The process facilitates a good and homogeneous dispersion of the particles into the inorganic matrix. The porous nature of the sol-gel derived amorphous silica matrix is an excellent host for supporting different types of guest nanoparticles which provides nucleation sites for magnetic nanoparticles and minimizes the aggregation imposing an upper limit to the size of the particles. This is the reason why the sol-gel synthesis method has gone an intensive development **[12-13]**.

In this paper, the influence of Zn-ferrite content on the electrical and dielectric properties of x ($ZnFe_2O_4$)/ (1-x) SiO_2 (where x=0.4, 0.6 and 0.8) nanocomposites prepared by sol-gel method has been reported aiming at tuning the dielectric properties of $ZnFe_2O_4$ nanoparticles dispersed in a silica matrix and greatly expanding the range of applications by adjusting the annealing temperature and $ZnFe_2O_4$ content.

2. Experimental Procedure:

The starting materials used in this work were Zn $(No_3)_2$.$6H_2O$, Fe $(No_3)_3$.$9H_2O$, urea, ethanol (ETOH) and tetraethylorthosilicate (TEOS). 0.2 M (50ml) of iron nitrate solution and 0.1 M (50ml) of zinc nitrate solution has been used and gelated by using 0.1M (300ml) of urea solution as a catalyst and distilled water as the solvent **[14]**. The TEOS: ETOH and Zn:Fe molar ratio were controlled at 1:4 and 1:2, respectively. The ratio of nanocomposites were x ($ZnFe_2O_4$)/ (1-x) SiO_2 (where x= 0.4, 0.6 and 0.8).

The two step sol-gel preparation method used is described in details **[14]**. A flowchart of the experimental procedure for the nano composites is reported in Fig. (1). Two separated solutions were prepared. In the first step, Ethanol and TEOS were mixed. The precursor solution was stirred for 1h at 75^oC when hydrolysis of TEOS took place **[15]**. In the second step, Iron nitrate solution and zinc nitrate solution was gelated by using urea solution as a catalyst and distilled water as the solvent. The solutions were stirred for 1h at 75^oC to form a homogeneous solution of zinc ferrite **[14]**. This solution was allowed to gel at 75^oC for 24h, obtaining an opaque white gel. The gels were inserted into an oven for further drying at 300^oC for 2h. They were then calcined at temperature 700, 800 and 900^oC in open atmosphere to form Zn-ferrite/ SiO_2 nanocomposites **[16]**.

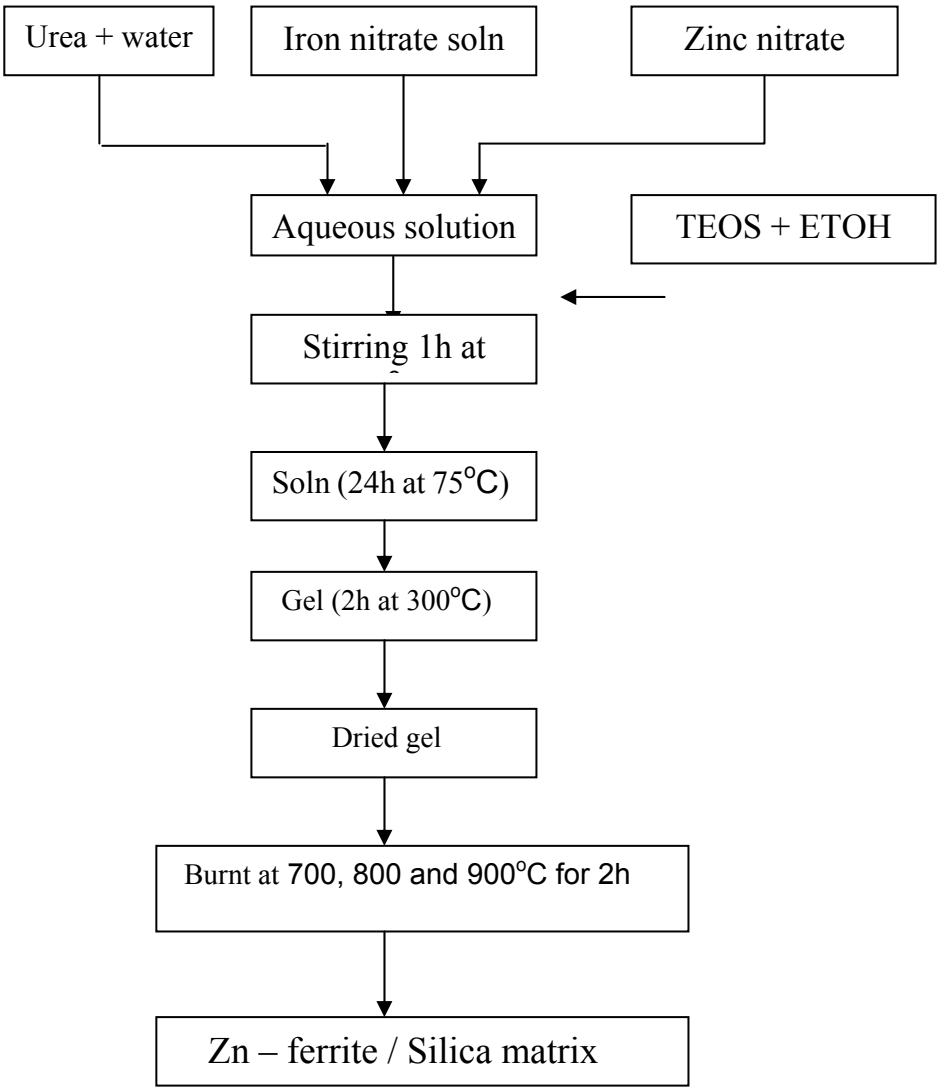

Fig.(1): Flowchart of the experimental procedure

The crystal phases were analyzed by X-ray diffractometer measured with radiations (λ= 1.54178Å) in the range 10°<2θ<80°. The TGA and DTA measurements were performed with a thermal detector (DTG-60H) at a heating rate of 10°C /min under open atmosphere in the temperature range of 50-1000°C. The electrical conductivity and dielectric measurements have been carried out in the frequency range 5 kHz to 100 kHz by using programmable automatic RLC (PM6304 Philips Bridge).

3. Results and Discussion:

3.1. Characterizations of the Samples:

The XRD patterns of the $ZnFe_2O_4$/ silica matrix samples sintered at 900^{o}C are shown in Fig. (2). These XRD patterns in the present investigation are compared with the corresponding standard patterns given in International Center for Diffraction Data (ICDD) files **[17]**. Diffraction peaks related to Zn-ferrite with spinel structure appeared and their sharpness and intensity are further enhanced with increasing ferrite content as a result of growing the ferrite phase. On the other hand, a secondary phase of ZnO was observed **[18]** which means that, the present composite is not a single phase even at high temperature. The average crystallite sizes of Zn-Ferrite in the amorphous silica matrix can be estimated from by using Scherrer formula **[19]**.

$$D= K\lambda / (\beta \cos\theta) \quad (1)$$

where D is the average crystallite size, K is a constant equal to 0.89; λ is the X-ray wave length (0.154 nm), β is the full width at half maximum (FWHM) and θ is the diffraction angle. The variation of the average particle size is from 5.17 nm to 34.6 nm for all samples annealed at different temperatures as shown in Table (1). The average particle size is found to increase with increasing of zinc ferrite content and annealing temperature.

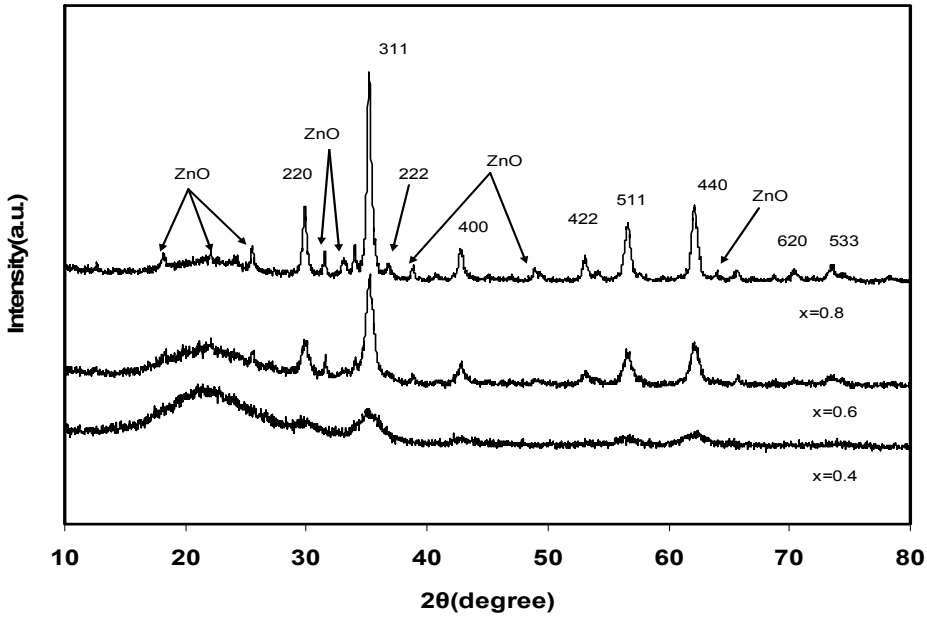

Fig.(2): XRD patterns of the samples annealed at 900°C.

Table (1): Average particle size of all samples

Annealing temperature	X=0.4	X=0.6	X=0.8
700 C°	5.17nm	8.62	12.9
800 C°	7.82	12.5	26
900 C°	10.3	17	34.7

Figure (3) shows the typical curves of the thermogravimetric analysis (TGA) of dried gel samples with different concentrations 0.4, 0.6 and 0.8 of Zn ferrites, in the temperature range of 50-1000^{o}C with heating rate of 10^{o}C / min. The weight loss profile shows three weight loss regions; the first one is due to the removal of surface water, the second is due to the decomposition of metal nitrates and the third one, at higher temperature is due to a gradual weight loss due to further removal of solvents, ethanol and embedded water from the pores. There was a little weight loss at temperature higher than 900^{o}C (thermal stability region) **[20]**. Also it is found that, the reaction temperate decreases by increasing Zn-ferrite content. Fig. (4) shows the Differential thermal analysis (DTA) curves of the dried gel samples, in temperature range of 50-1000^{o}C with heating rate of 10^{o}C /min. At relatively low temperatures, endothermic process occurs which is due to removing trapped water, surface water and organic residues. At relatively higher temperatures, there was no other thermal processes occur in agreement with TGA in these regions of thermal stability.

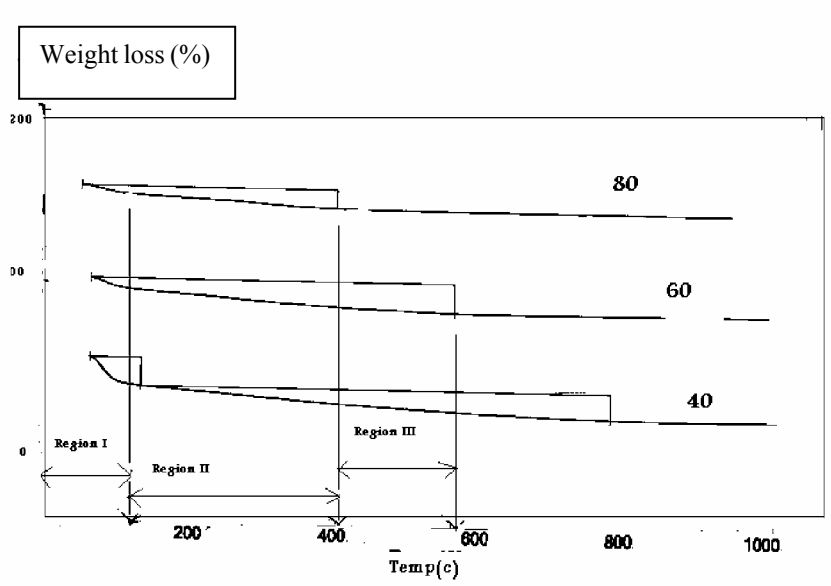

Fig.(3): The TGA curves of dried gel samples of different Zn-ferrite concentration .

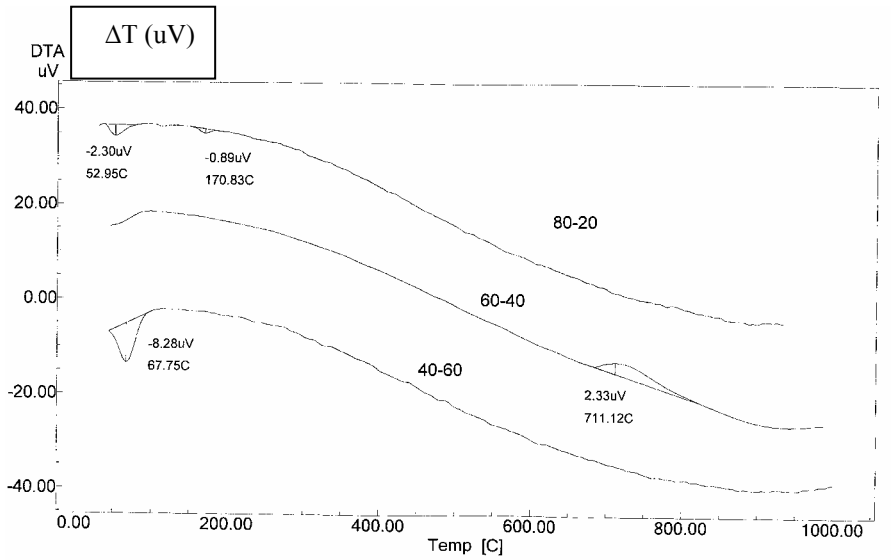

Fig.(4): The DTA curves of dried gel samples of different Zn-ferrite concentration .

3.2 Compositional Variation of ρ, ε'

The electrical resistivity at room temperature of the different annealed samples at 100 kHz is shown in Fig. (5). It is seen that when zinc-ferrite embedded in silica increases, the electrical resistivity increases as well as with increasing annealing temperature. Similar results were reported by Mesh Kumar et al. [21] for electrical resistivity as a function of annealing temperature. The improvement of electrical resistivity is attributed to the large grain boundaries **[21]**.

It can also be seen from Fig. (5) that the electrical resistivity of the samples increases with increasing zinc-ferrite content, for the samples annealed at 700,800 and 900°C. The electrical conduction in ferrites, in general, can be explained by the Verwey mechanism of electron hopping between cations with two different valance states distributed randomly on equivalent lattice sites **[22]**. Occurrence of ions in more than one valence states is caused by the preparation conditions, annealing temperature, sintering atmosphere and sintering time. According to this model, ferrites are known to form a close packed oxygen (anions) lattice with the metal ions (cations) situated at tetrahedral sites (A-sites) and the octahedral sites (B-sites). These cations can be well treated as isolated from each other, to a first approximation. Here, the conduction mechanism may be explained based on the hopping of electrons between Fe^{2+} and Fe^{3+} ions at B-sites **[22, 23].**

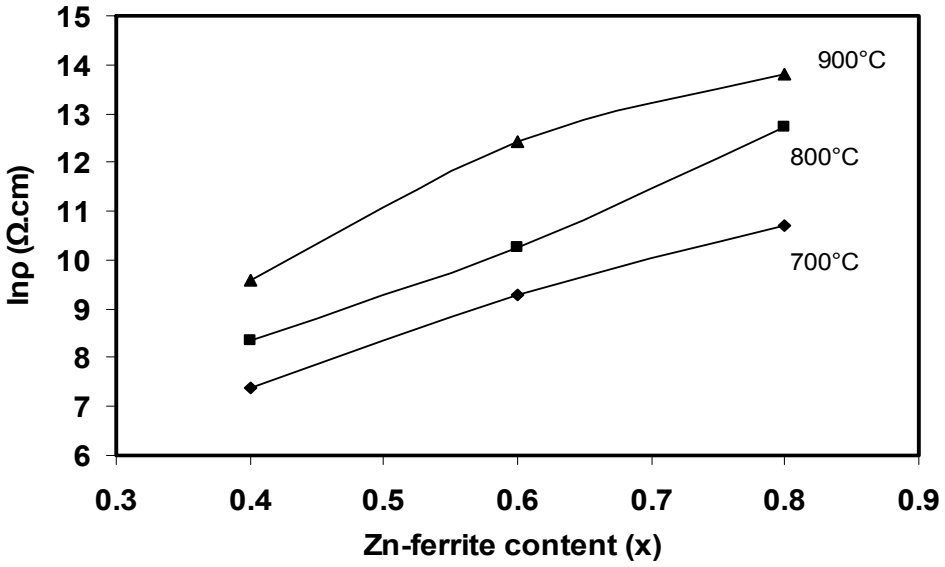

Fig.(5): Variation of electrical resistivity with zinc-ferrite content for samples annealed at 700,800 and 900°C.

The resistivity and dielectric constant are important parameters of the ferrites from the application point of view. The variation of dielectric constant at 100 kHz frequency of the samples, sintered at 700,800 and 900°C, as a function of zinc-ferrite content is shown in Fig.(6). It is clear from Figs. (5) and (6), that the variations of resistivity and dielectric constant as a function of zinc-ferrite content are having opposite trends with each other. A similar trend was reported by several authors in the case of Li–Cd ferrites and Shaikh et al. **[26]** in Li–Mg–Zn ferrites. Iwauchi **[27]** and Rezlescu **[28]** established a strong correlation between the conduction mechanism and dielectric behavior of ferrites. They have concluded that the electronic exchange between Fe^{2+} and Fe^{3+} results in the local displacement of charges in the direction of the applied electric field which determines the polarization in the ferrites. The magnitude of exchange depends upon the concentration of Fe^{2+}/Fe^{3+} ion pairs present on B-site. The increase in the electrical resistivity with increasing zinc-ferrite concentration may be attributed to the relative decrease of Fe^{2+} concentration at B-sites **[24]**.

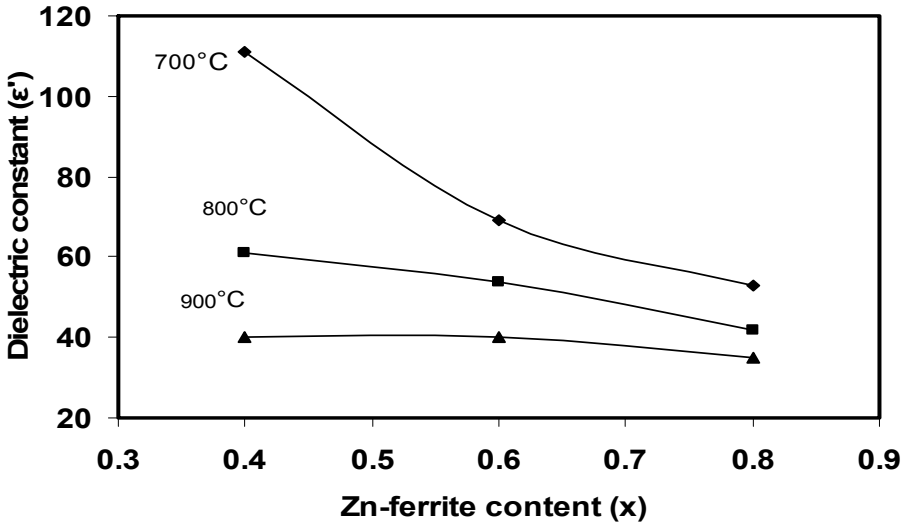

Fig.(6): Variation of dielectric constant with zinc-ferrite content for samples annealed at 700,800 and 900°C.

3.3. Temperature Dependence of the Electrical Conductivity:

Temperature dependence on conductivity for the present samples was studied over the temperature range from room temperature to 300°C. For example, zinc-ferrite sample, x=0.8 annealed at 800°C is shown in Fig. (7). The conductivity is found to increase with increasing temperature for all the studied samples. This could be attributed to the increase in the drift mobility of electric charge carriers which are thermally activated on increasing the temperature **[29]**. The observed behavior of increasing conductivity with increasing temperature clearly indicates that the present of zinc-ferrite in silica has semiconductor like behavior.

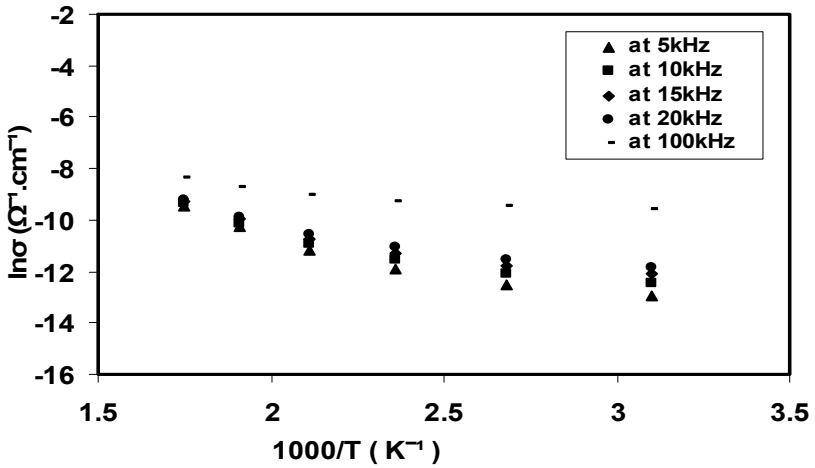

Fig.(7): Temperature dependence of electrical conductivity of sample of x=0.8 zinc-ferrite annealed at 800°C.

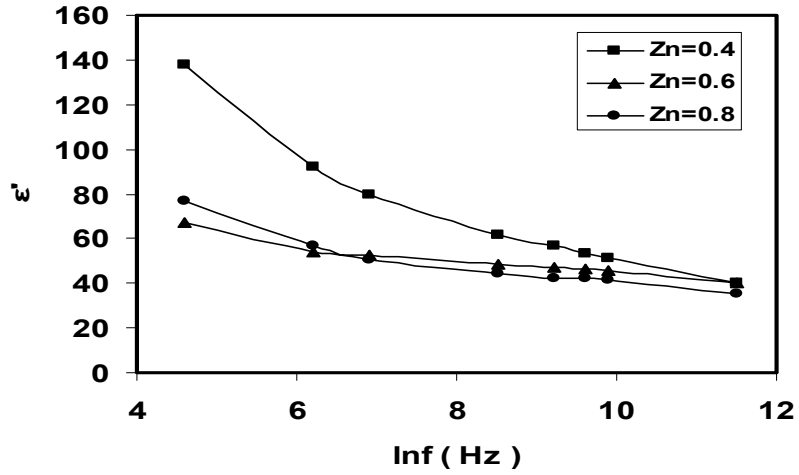

Fig.(8): Variation of dielectric constant ε' with frequency for samples annealed 900

3.4. Frequency dependence of the dielectric constant

The frequency dependence of the real part of the dielectric constant ε' was studied, at room temperature, with frequency ranges 5-100 kHz. For samples annealed at 900°C is shown in Fig. (8). As seen from the figure, the dielectric constant is found to decrease with increasing in frequency for all the samples. The decrease is rapid at lower frequencies and slower at higher frequencies. This kind of decrease in dielectric constant with increasing frequency is a

normal dielectric behavior and was observed by several other investigators **[30,31]**. Earlier, Iwauchi **[27]** and Rezlescu **[28]** concluded that electron exchange between Fe^{2+} and Fe^{3+} results in local displacement of charges and are responsible for the dielectric behavior in ferrites. At higher frequencies the electron exchange between ferrous and ferric ions cannot follow the alternating field, which causes a decrease in the contribution of interfacial polarization to dielectric constant, and thus we see a decrease in the dielectric constant at higher frequencies **[30]**.

4. Conclusions:

In the present work the influence of Zn-ferrite content on the electrical and dielectric properties of x (ZnFe2O4)/ (1-x) SiO2 (where x= 0.4, 0.6 and 0.8) nanocomposites prepared by sol-gel method was studied. The study of electrical resistivity of the samples shows that the resistivity increases with increasing Zn-ferrite content, whereas the dielectric constant of the samples is found to decrease with increasing Zn-ferrite content. The temperature variation of electrical conductivity shows that the conductivity increases with increasing temperature .The dielectric constant of the samples is found to decrease with the increase in frequency. This is attributed to the decrease in the contribution of interfacial polarization at higher frequencies, as at higher frequencies the electron exchange between ferrous and ferric ions cannot follow the alternating field.

References:

1. B. Baruwati, K. Reddy, S. Manorama, R. Singh, O. Parkash, *Appl. Phys*. Lett. **85,** 2833 (2004).

2. J. Smit, H.P.J. Wijn, Ferrites, in: N.V. Philips, (Ed.), Philips Technical Library, Eindhoven, The Netherlands, (1959).

3. P. Vijaya Bhasker Reddy, B.Ramesh, Ch.GopalReddy, Physica B **405**, 1852 (2010).

4. D.W. Johnson, B.B. Ghate, F.Y. Wang, Advances in Ceramics, *American Ceramic Society, Columbus*, OH, vol. **15**, p. 27 (1985).

5. E. Veena Gopalan, P.A. Joy, I.A. Al-Omari, D. Sakthi Kumar, Y. Yoshida, M.R. Anantharaman, *J. Alloys Compd*. **485**, 711 (2009).

6. Y. Wang, G. Xu, L. Yang, Z. Ren, X. Wei, W. Weng, P. Du, G. Shen, G. Han, *Ceram. Int*. 35 (2009) 1285.

7. P. Priyadharsini, A. Pradeep, G. Chandrasekaran, *J. Magn. Magn. Mater*. **321**, 1898 (2009).

8. J. Wang, P.F. Chong, S.C. Ng, L.M. Gan, *Mater. Lett*. **30**, 217 (1997).

9. P. Ravindranathan, K.C. Patil, *Am. Ceram. Soc. Bull*. **66**, 688 (1987).
10. V. Pillai, D.O. Shah, *J. Magn. Magn. Mater*. **163**, 243 (1996).
11. M. Lal, D.K. Sharma, M. Singh, Indian *J. Pure Appl. Phys*. **43**, 291 (2005).
12. M. Sedlar, V. Matejec, T. Grygar, *J. Kadlekova, Cer. Int*. **26**, 507 (2000).
13. K.H.Wu,W.C. Huang, *J. Solid State Chem*. **177**, 3052 (2004).
14. L.A. Garcia-Cerda, V.A. Torres-Garcia, J.A.Matutes-Aquino, O.E. Ayala
15. Valenzuela, *J. Alloys and Compounds*, **369**, 148 (2004).
16. Shifeng Yan, Jianxin Geng, Jianfeng Chen, Li Yin, Yunchun Zhou, Leijing Liu, Enle Zhou, *J. Magn. Magn. Mater*. **292**, 304 (2005).
17. M.Atif, S.K.Hasanain, M. Nadeem, *Solid State Comm*. **138**, 416 (2006).
18. M. Stefanescu, C. Caizer, M. Stoia, O. Stefanescu, *Acta Mater*. **54**, 1249 (2006).
19. Z.H.Zhou, J. M.Xue, J. Wang, *J. Appl. Phys*., **91**, 6015 (2002).
20. G. Xiong, M. Xu, Z.H. Mai, *Solid State Comm*. **118**, 53 (2001).
21. R. Murugaraj, G. Govindaraj and D.George, *Mater. Let*. **57**, 1656 (2003).
22. Mahesh Kumar, M. Chaitanya Varma, C.L. Dube, K.H. Rao, S.C. Kashyap, *J. Magn. Magn. Mater*. **320**, 1995 (2008).
23. E.J.W. Verway, P.W. Haayman, *Physica* **8**, 979 (1941).
24. D. Kothari, S. Phanjoubam, J.S. Baijal, *J. Mater. Sci.* **25**, 5142 (1990).
25. Hosseinpour, H. Sadeghi, A. Morisako, *J. Magn. Magn. Mater*. **316**, 283 (2007).
26. S.C. Watawe, U.A. Bamne, S.P. Gonbare, R.B. Tangsal, *J. Mater. Chem. Phys*. **103**, 323 (2007).
27. A.M. Shaikh, S.S. Bellad, B.K. Chougule, *J. Magn. Magn. Mater*. **195**, 384 (1999).
28. K. Iwauchi, Japan. *J. Appl. Phys*. **10**, 1520 (1971).
29. N. Rezlescu, E. Rezlescu, *Phys. Stat. Sol*. (a) **23**, 575 (1974).
30. M. El-Shabasy, *J. Magn. Magn. Mater*. **172**, 188 (1997).
31. M.R. Ananthraman, S. Sindhu, S. Jagatheesan, K.A. Malini, P. Kurian, *J. Phys*. D **32**, 1801 (1999).
32. R.V. Magalaraja, S. Ananthakumar, P. Manohar, F.D. Gnanam, *J. Magn. Magn. Mater*. 253, 56 (2002).